ICA-enabled oxygen-enhanced MRI (OE-MRI) correlates with pulmonary function tests in cystic fibrosis

Sarah H. Needleman[1], Mina Kim[1], Jamie R. McClelland[1], Marta Tibiletti[2], Christopher Short[3,4,5], Thomas Semple[3,4], Jane C. Davies[3,4,5], and Geoff J. M. Parker[1,2]

[1]Centre for Medical Image Computing (CMIC), Department of Medical Physics & Biomedical Engineering, University College London, London, United Kingdom, [2]Bioxydyn Limited, Manchester, United Kingdom, [3]National Heart & Lung Institute, Imperial College London, London, United Kingdom, [4]Royal Brompton Hospital, Guy's & St Thomas' Trust, London, United Kingdom, [5]European CF Society Lung Clearance Index Core Facility, London, United Kingdom

Synopsis

Keywords: Lung, Data Processing

Motivation: There is a clinical need for non-ionising methods to assess heterogeneous lung function in cystic fibrosis (CF). Dynamic oxygen-enhanced MRI (OE-MRI) can assess regional lung function, however OE-MRI analysis is impaired by confounding signals and poor SNR.

Goal(s): To evaluate the sensitivity of OE-MRI measures to the lung clearance index (LCI) in CF, with and without independent component analysis (ICA) to reduce noise.

Approach: We used ICA to reduce noise in the OE-MRI measures. We evaluated the correlation between OE-MRI measures, LCI, and pulmonary function tests.

Results: OE-MRI measures demonstrated significant correlation with LCI. OE-MRI measures extracted using ICA displayed clear oxygen-enhancement responses.

Impact: Dynamic lung OE-MRI measures extracted using independent component analysis (ICA) exhibited significant correlation with lung clearance index ($LCI_{2.5}$) in cystic fibrosis (CF) patients, suggesting a potential application of ICA-extracted OE-MRI measures to assess regional disease severity in CF.

Introduction

Dynamic oxygen-enhanced MRI (OE-MRI) uses inhaled oxygen to provide contrast to indicate regional lung function. T_2^*-sensitive dual-echo dynamic lung OE-MRI acquisitions have recently been demonstrated at 3T[1] and 1.5T[2]. However, analysis of dynamic lung OE-MRI is challenging due to the presence of artefacts, confounding signals, and poor SNR. Application of independent component analysis (ICA) to dynamic lung OE-MRI can separate the lung's oxygen-enhancement response from confounds[3]. Here we present the application of ICA to dual-echo dynamic OE-MRI in cystic fibrosis (CF). We examine the correlation between dynamic OE-MRI, the lung clearance index and spirometry.

Methods

11 CF patients (median age 26 years, range 8-46) were imaged using a free-breathing dynamic 2D multi-slice dual-echo RF-spoiled gradient echo OE-MRI acquisition at 1.5T[2] (sequence parameters are provided in Table 1). Subjects inhaled medical air (approximately 1.5 minutes), 100% oxygen (approximately 3.5 minutes), and medical air (approximately 4 minutes) via a non-rebreathing mask.

The dynamic MRI series were registered using NiftyReg[3,4]; density-induced MR signal alterations were not corrected. A median filter[5] was applied to each echo using a 3x3x3 kernel (in-plane spatial and temporal filtering).

R_2^* and S_0 were extracted from the dual-echo data within a cardiac mask consisting of cardiac tissue, lung tissue, and major blood vessels, assuming a monoexponential signal decay. ICA was applied to separate the oxygen-enhancement response of R_2^* and S_0 from confounding signals using the pipeline described by Needleman et al.[3]. The pipeline was altered for application to R_2^* and S_0 and a single oxygen-inhalation period by considering 2-72 ICA components. ΔR_2^* and ΔS_0 were calculated as the difference between 100% oxygen-inhalation (average over 180-215 dynamics) and air-inhalation (average over 10-50 dynamics). ΔR_2^* and ΔS_0 were calculated for the registered MRI data without application of ICA ($\Delta R_{2\ MRI}^*$ and $\Delta S_{0,MRI}$) and for the ICA-extracted parameters ($\Delta R_{2\ ICA}^*$ and $\Delta S_{0,ICA}$).

Subjects underwent pulmonary function testing (PFT) using spirometry to obtain FEV1 %predicted (FEV1%p) and FVC %predicted (FVC%p), and multiple breath N_2 washout to obtain the lung clearance index ($LCI_{2.5}$). The median lung values of $\Delta R_{2\ MRI}^*$, $\Delta R_{2\ ICA}^*$, $\Delta S_{0,MRI}$, and $\Delta S_{0,ICA}$ were compared with the PFT measures using Pearson's correlation; $p < 0.05$ was considered significant.

Results

The ICA-derived time series $\Delta R_{2\ ICA}^*$ and $\Delta S_{0,ICA}$ (Figure 1(Aii,iv),(Bii,iv)) demonstrated clearer oxygen-enhancement with reduced signal fluctuations than were observed in $\Delta R_{2\ MRI}^*$ and $\Delta S_{0,MRI}$ (Figure 1(Ai,iii),(Bi,iii)). The $\Delta R_{2\ ICA}^*$ maps of a CF patient ($LCI_{2.5}$ 11.4), shown in Figure 2(Aiii), exhibited homogeneous positive $\Delta R_{2\ ICA}^*$ in lung tissue and weakly negative $\Delta R_{2\ ICA}^*$ in the heart and aorta. The subject's $\Delta S_{0,ICA}$ maps (Figure 2(Av)) demonstrated positive $\Delta S_{0,ICA}$ in lung tissue; positive and negative $\Delta S_{0,ICA}$ was observed in cardiac tissue and vessels. The $\Delta R_{2\ ICA}^*$ and $\Delta S_{0,ICA}$ maps of a patient with higher $LCI_{2.5}$ (19.6) (Figure 2(Biii,v)) appeared heterogeneous.

$\Delta R_{2\ MRI}^*$, $\Delta R_{2\ ICA}^*$, $\Delta S_{0,MRI}$, $\Delta S_{0,ICA}$ exhibited significant correlations with $LCI_{2.5}$ (Table 2). $\Delta R_{2\ MRI}^*$ and $\Delta R_{2\ ICA}^*$ also displayed significant correlations with FEV1%p and FVC%p, but $\Delta S_{0,MRI}$ and $\Delta S_{0,ICA}$ did not. The ICA-derived $\Delta R_{2\ ICA}^*$ and $\Delta S_{0,ICA}$ displayed a stronger correlation with $LCI_{2.5}$ than those calculated directly from the MRI data (scatter plots are presented in Figure 3).

Discussion

The reduced signal fluctuations of the $\Delta R_{2\ ICA}^*$ and $\Delta S_{0,ICA}$ time series suggests ICA was effective in reducing confounds.

$LCI_{2.5}$ is of interest as a global marker of CF disease severity, particularly for early disease[6]. OE-MRI biomarkers provide regional lung function measures, of relevance to heterogeneous presentations of CF. All OE-MRI measures exhibited significant correlations with $LCI_{2.5}$, with greater correlations demonstrated by the ICA-derived OE-MRI measures, suggesting a likely sensitivity to CF disease severity and the benefits of applying ICA.

ΔR_2^* is potentially more specific to ventilation than ΔS_0, as lung ΔR_2^* is driven by magnetic susceptibility changes arising from an increased concentration of gaseous oxygen[3,7]. The strong relation of $\Delta R_{2\ ICA}^*$ to ventilation likely resulted in its good correlation with PFTs.

ΔS_0 in a spoiled gradient echo is influenced by proton density and R_1; ΔR_1 is driven by changes in the concentration of dissolved oxygen in lung tissue water and blood plasma, which reflects the combination of ventilation, diffusion, and perfusion[3,8]. The lower correlation of $\Delta S_{0,ICA}$ than $\Delta R_{2\ ICA}^*$ with PFTs may be due to the influence of gas exchange and perfusion on $\Delta S_{0,ICA}$, which is not reflected in the functional measurements available in this study. The influence of proton density variation is also likely to confound ΔS_0 more than ΔR_2^*.

Conclusion

The oxygen-induced change of R_2^* and S_0 (a parameter relating to R_1), derived from dual-echo gradient echo dynamic OE-MRI, demonstrated good correlation with lung clearance index in cystic fibrosis, suggesting a potential sensitivity to disease severity. ICA increased the sensitivity of the method.

Acknowledgements

This work is supported by the EPSRC-funded UCL Centre for Doctoral Training in Medical Imaging (EP/L016478/1), by the Cancer Research UK National Cancer Imaging Translational Accelerator (NCITA) award C1519/A28682, by Innovate UK award 104629, by Cystic Fibrosis Foundation, grant number 0208A120, and by the NIHR Imperial Biomedical Research Centre. JM acknowledges funding from CRUK via the Network Accelerator Award Grant (A21993) to the ART-NET consortium and the Wellcome/EPSRC Centre for Interventional and Surgical Sciences (WEISS) (203145/Z/16/Z).

References

1. Kim M, Naish JH, Needleman SH, et al. Feasibility of dynamic T2*-based oxygen-enhanced lung MRI at 3 T. *Magn Reson Med*. Published online 2023:1-15. doi:10.1002/mrm.29914

2. Tibiletti M, Short C, Naish JH, et al. Double-echo Oxygen Enhanced MRI at 1 . 5 T correlates with clinical lung function in CF patients. In: *Proc. Intl. Soc. Mag. Reson. Med. 32.* ; 2023:1399. doi:10.3389/fninf.2014.00044.4

3. Needleman SH, Kim M, McClelland JR, et al. Independent component analysis (ICA) applied to dynamic oxygen-enhanced MRI (OE-MRI) for robust functional lung imaging at 3 T. *Magn Reson Med*. Published online 2023:1-17. doi:10.1002/mrm.29912

4. Modat M, Ridgway GR, Taylor ZA, et al. Fast free-form deformation using graphics processing units. *Comput Methods Programs Biomed*. 2010;98(3):278-284. doi:10.1016/j.cmpb.2009.09.002

5. van der Walt S, Schönberger JL, Nunez-Iglesias J, et al. scikit-image: image processing in Python. *PeerJ*. 2014;2:e453. doi:10.7717/peerj.453

6. Davies JC, Cunningham S, Alton EWFW, Innes JA. Lung clearance index in CF: a sensitive marker of lung disease severity. *Thorax*. 2008;63(2):96 LP - 97. doi:10.1136/thx.2007.082768

7. Pracht ED, Arnold JFTT, Wang T, Jakob PM. Oxygen-enhanced proton imaging of the human lung using T2*. *Magn Reson Med*. 2005;53(5):1193-1196. doi:10.1002/mrm.20448

8. Edelman RR, Hatabu H, Tadamura E, Li W, Prasad P V. Noninvasive assessment of regional ventilation in the human lung using oxygen–enhanced magnetic resonance imaging. *Nat Med*. 1996;2(11):1236-1239. doi:10.1038/nm1196-1236

Figures

TEs (ms)	0.98, 2.0	Number of coronal slices	5
TR (ms)	16	Slice thickness (mm)	10
Flip angle (degrees)	5	Field of view (mm^2)	450 x 450
Number of dynamic images	360	2D pixel dimensions (mm^2)	4.7 x 4.7
Acquisition duration (minutes)	9	Temporal resolution (s)	1.5

Table 1: Sequence parameters of the free-breathing dynamic 2D multi-slice dual-echo RF-spoiled gradient echo (T1-FFE) OE-MRI acquisition at 1.5T[2].

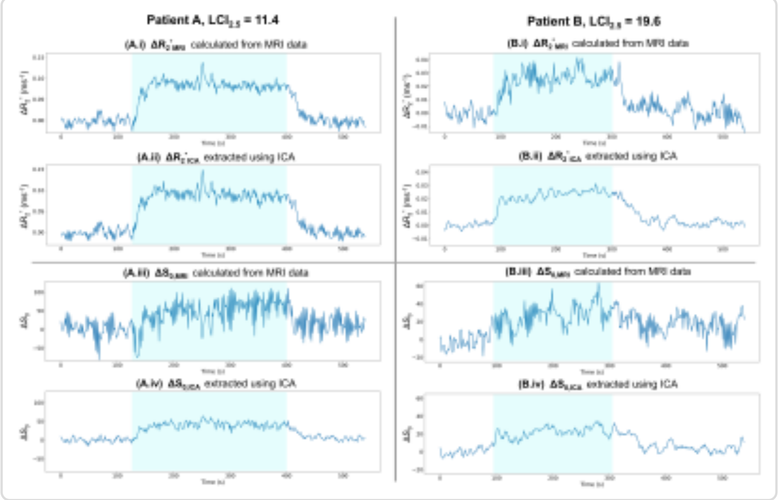

Figure 1: Time series of the median lung value of (i) $\Delta R_{2\ MRI}^*$, (ii) $\Delta R_{2\ ICA}^*$, (iii) $\Delta S_{0,MRI}$, and (iv) $\Delta S_{0,ICA}$ for two CF patients: (A) 19 years, $LCI_{2.5}$ = 11.4, FEV1p% = 96, FVCp% = 112, and (B) 46 years, $LCI_{2.5}$ = 19.6, FEV1p% = 51, FVCp% = 58. Subject (B) exhibited lower amplitudes than subject (A). The time series extracted from the MRI data (i, iii) contained artefactual signal fluctuations which were reduced in the time series extracted using ICA (ii, iv). The ICA-extracted time series displayed well-defined oxygen-enhancement responses. Blue shading indicates 100% oxygen inhalation.

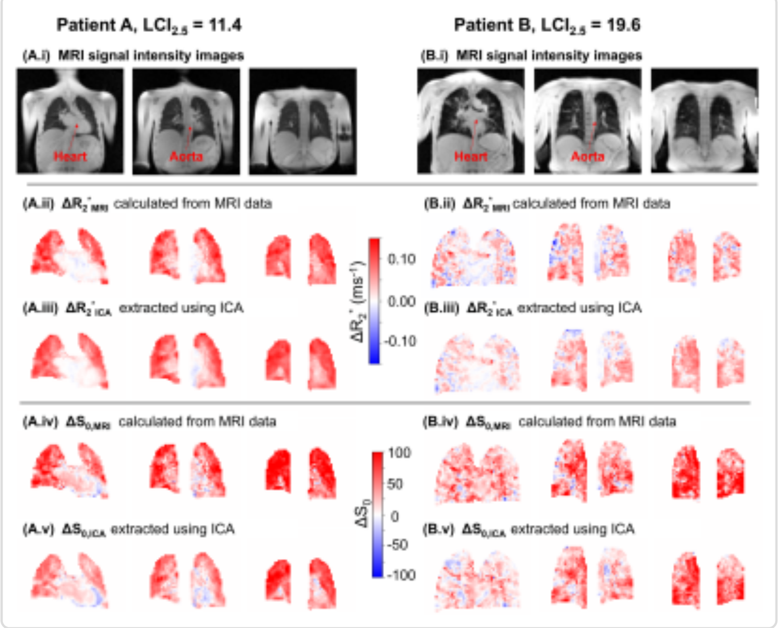

Figure 2: (i) MRI images, and maps of (ii) $\Delta R_{2\ MRI}^*$, (iii) $\Delta R_{2\ ICA}^*$, (iv) $\Delta S_{0,MRI}$, and (v) $\Delta S_{0,ICA}$ for three coronal slices from the two CF patients in Figure 1. Subject (A) demonstrated homogeneous positive $\Delta R_{2\ ICA}^*$ in lung tissue; cardiac tissue and the aorta displayed a weakly negative $\Delta R_{2\ ICA}^*$. Subject (A) demonstrated positive $\Delta S_{0,ICA}$ in lung tissue with regions of negative $\Delta S_{0,ICA}$ in cardiac tissue and vessels. The lung appeared heterogeneous in both $\Delta R_{2\ ICA}^*$ and $\Delta S_{0,ICA}$ for subject (B). The lung appeared more homogeneous in $\Delta R_{2\ ICA}^*$ and $\Delta S_{0,ICA}$ than $\Delta R_{2\ MRI}^*$ and $\Delta S_{0,MRI}$ for subject (A).

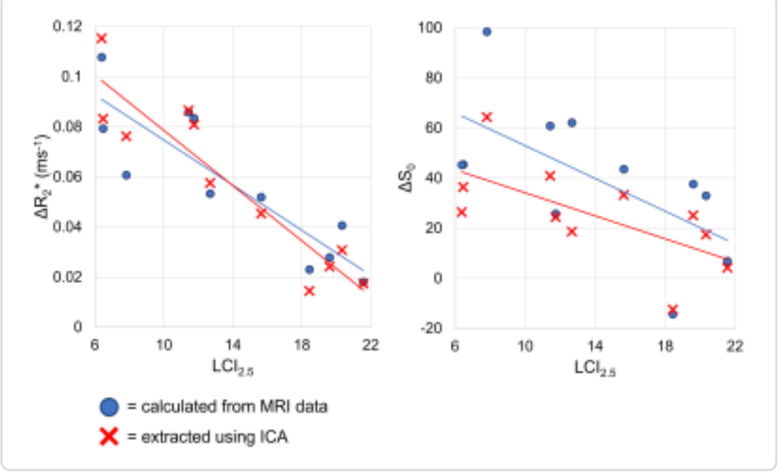

Figure 3: Scatter plots of the linear correlation between ΔR_2^* (left) and ΔS_0 (right) with lung clearance index ($LCI_{2.5}$). Both the ICA-extracted measures ($\Delta R_{2\ ICA}^*$ and $\Delta S_{0,ICA}$, red) and the measures calculated from registered MRI data without application of ICA ($\Delta R_{2\ MRI}^*$ and $\Delta S_{0,MRI}$, blue) are shown.

	$LCI_{2.5}$	FEV1%p	FVC%p
$\Delta R_{2\ MRI}^*$ (ms^{-1})	-0.87 (**$p < 0.001$**)	0.95 (**$p < 0.001$**)	0.83 (**$p = 0.002$**)
$\Delta R_{2\ ICA}^*$ (ms^{-1})	-0.93 (**$p < 0.001$**)	0.94 (**$p < 0.001$**)	0.80 (**$p = 0.003$**)
$\Delta S_{0,MRI}$	-0.62 (**$p = 0.041$**)	0.52 ($p = 0.105$)	0.31 ($p = 0.359$)
$\Delta S_{0,ICA}$	-0.65 (**$p = 0.030$**)	0.53 ($p = 0.094$)	0.32 ($p = 0.339$)

Table 2: Pearson's correlation of the dynamic OE-MRI measures ($\Delta R_{2\ MRI}^*$, $\Delta R_{2\ ICA}^*$, $\Delta S_{0,MRI}$, $\Delta S_{0,ICA}$) with PFTs. OE-MRI measures extracted using ICA ($\Delta R_{2\ ICA}^*$ and $\Delta S_{0,ICA}$) are shaded in blue.